A microfluidic column of water index-matched packed microspheres for label-free observation of water pollutants

Roberta Lanfranco [a], Janire Saez [b], Deborah Abati [a], Thomas Carzaniga [a], Fernando Benito-Lopez [b,*], Marco Buscaglia [a,*]

[a] Department of Medical Biotechnology and Translational Medicine, University of Milan, via F.lli Cervi 93, 20054, Segrate (MI), Italy
[b] Microfluidics Cluster UPV/EHU, Analytical Microsystems & Materials for Lab-on-a-Chip (AMMa-LOAC) Group, Analytical Chemistry Department, University of the Basque Country UPV/EHU, Barrio Sarriena s/n 48940 Leioa, Spain
[*]Corresponding authors: marco.buscaglia@unimi.it (M. Buscaglia, via F.lli Cervi 93, 20090 Segrate, Italy), fernando.benito@ehu.eus (F. Benito-Lopez, Paseo de la Universidad, 7, 01006, Vitoria-Gasteiz, Spain)

Abstract

A microfluidic, label-free optical sensor for water pollutants, which is based on a packed micro-column of microspheres with refractive index similar to that of water, is presented. The perfluoropolyether microspheres are synthetized by membrane emulsification followed by UV irradiation. The microfluidic channel hosting the packed column is transparent when filled with pure water as a consequence of refractive index matching, whereas it scatters light in presence of compounds with lipophilic moieties that spontaneously adsorb on the fluorinated microspheres. The device is characterized by analysing the response to cationic and anionic surfactants. Both the signal growth rate and the recovery rate measured during washing with water depend on the type and concentration of the compounds. The cationic surfactant displays a larger signal increase, linearly scaling with concentration. A limit of detection of 1 μM is obtained in the current configuration. The water index-matched microspheres enable to access an additional analytical parameter, that is the propagation velocity of the scattering signal along the column. This parameter is also found to scale linearly with concentration, hence providing a complementary analytical tool sensitive to the adhesion kinetics.

Keywords: microfluidic device; label-free optical sensor; reflective phantom interface; scattering phantom interface; water index-matched materials; environmental monitoring.

Introduction

Water pollution is a constant concern worldwide being oils and surfactants especially harmful for human health and the environment. Therefore, they should be continually monitored to avoid spread of contamination. The toxicity of surfactants varies between compounds and organisms [1]. Maximum allowed concentrations of anionic and non-ionic surfactants that can be released in aquatic basins are of the order of 1 μg mL^{-1}, whereas limits for cationic surfactants can be smaller, down to 0.2 μg mL^{-1}. These limits are about one order of magnitude larger for release in sewage systems. To assess these pollutants, liquid chromatography represents the gold standard in centralized laboratories. However, this technique is typically expensive, requires time consuming processes and is not suitable for on-site monitoring [2]. In this sense, miniaturized liquid chromatography in microfluidics has been proven to provide rapid separations with smaller consumption of sample and reagents, being suitable for integration into remote, autonomous analytical platforms for the monitoring of water pollutants [3]. Miniaturized separation devices have been proposed in the form of either lateral flow membrane systems [4] or packed column of microspheres [5][6], with applications in cell capture and analysis [7][8], antibody separation [9], and nucleic acids detection [10][11]. Another potential advantage is the visualization of analytes binding/unbinding within the porous medium by optical imaging techniques, which have been shown to provide a more detailed understanding of the binding process [12]. Similarly, affinity and

kinetics of microRNA hybridization targets confined in a nanofluidic channel have been measured from the analysis of time-resolved binding profiles on a long biosensor surface [13]. However, in these examples, the signal was provided by fluorescence, hence increasing the complexity of preparation and limiting the applicability of the methods. In contrast, label-free detection methods do not require any labelling of the analytes and can be virtually applied to any class of target molecules. Nevertheless, the surface structure of a packed column of microspheres is not compatible with most optical label-free approaches, which typically require an extended planar surface, possibly patterned with regular micro- or nano-structures [14]. A particularly simple and flexible approach is represented by the Reflective Phantom Interface (RPI) optical detection method [15][16], in which the signal arises from the formation of a thin molecular layer of analytes on a planar interface with very low reflectivity. The RPI method has been previously exploited to capture molecular targets by immobilized ligands [17][18][19][20], as well as to characterize the adsorption strength and kinetics on the surface of a prism of perfluorinated material that matches water's refractive index [21]. An analogous strategy, named as Scattering Phantom Interface (SPI) method [14][21][22], can be exploited to measure the amount of molecules binding on the internal surface of a micro-porous medium with refractive index similar to that of the liquid phase. This approach is based on a fundamental principle of optics: a collection of molecules freely diffusing in solution provides a very small light scattering, whereas the same amount of molecules confined at an interface with micron-scale curvature yields to a much larger scattering contribution [23].

In this work, we present the design, characterization, and performance of a miniaturized device, composed by a packed column of water index-matched (WIM) micro-spheres hosted in a microfluidic channel, which enables the label-free optical measurement of molecular binding of surfactants by SPI. The device provides access to real-time binding profiles along the column without the need of labelling the analytes, and offers a larger set of characterization parameters, through the visualization of the analyte binding in flow, within the column.

2. Materials and Methods

2.1 Perfluoropolymers microspheres production

The WIM micro-spheres were produced by photo-polymerization of a micro-emulsion containing a dispersed phase composed by a mixture of 70 % (w/v) Fomblin MD40® and 30 % (w/v) Fomblin MD700® (Solvay Specialty Polymers, Italy, www.solvay.com), and a continuous phase of 4 % (w/v) sodium dodecyl sulphate (SDS) (Sigma-Aldrich, USA, www.sigmaaldrich.com) solution in water. More details on the selection of materials and the production of the microspheres are provided as Electronic Supporting Material (ESM), section S1. The fluorinated oils contained 0.1 % (w/v) Ciba Irgacure 651® (Ciba Specialty Chemicals, Switzerland) as photoinitiator to start the polymerization reaction. After polymerization, the microspheres stability was tested through cycles of drying/wetting with ethanol and water before the insertion into the microfluidic device. Microspheres samples maintained their shape and size after repeated cycles, as well as after long-term storage. The size of the microspheres was measured by analyzing optical microscopy images through ImageJ (Figure 1a-b).
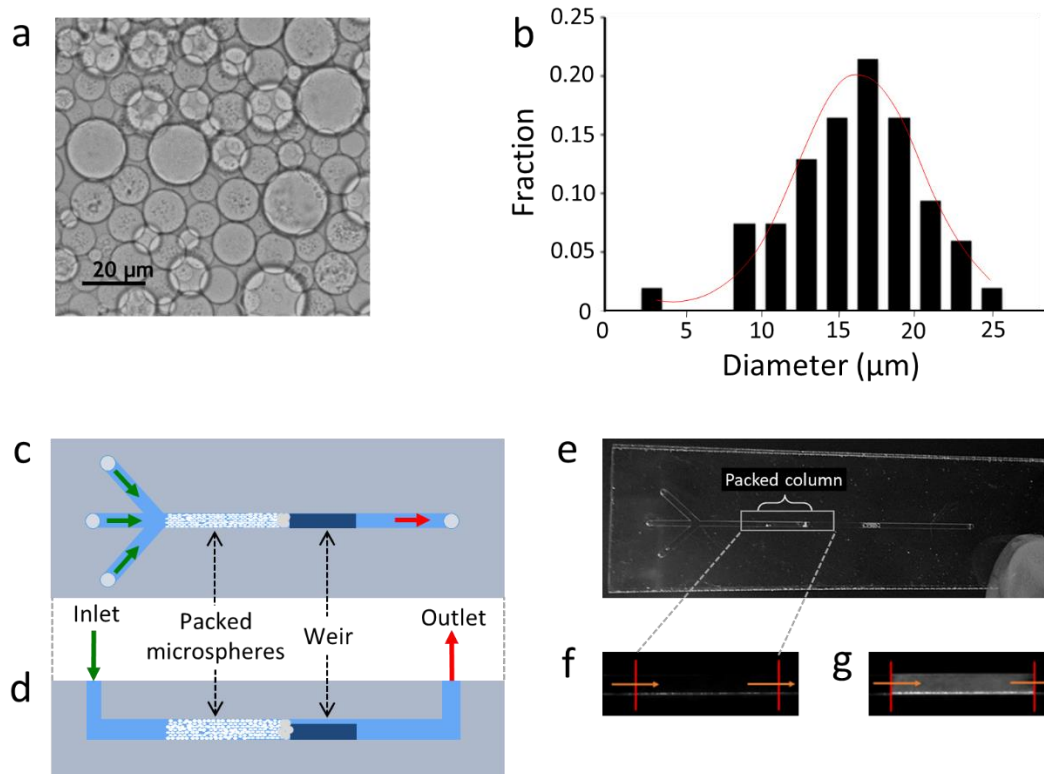
Figure 1. Scheme and pictures of the microfluidic device hosting the phantom microspheres. (a) Microscope image of the microspheres. (b) Size distribution of the microspheres. (c) Top view of the microfluidic device hosting the packed column. (d) Side section scheme of the microfluidic device. (e) Image of the fabricated device. Enlarged view of the part hosting the microspheres soaked with (f) deionized water ($n_s = 1.333 \pm 0.001$) and with (g) a NaCl 750 mM water solution ($n_s = 1.340 \pm 0.001$).

2.2 Microfluidic device fabrication

The microfluidic device was fabricated using a multilayer technique, as described in a previous work [24]. Briefly, five 100 μm layers of cyclo olefin polymer (COP, Zeonor COP sheets purchased from Zeonex, Germany, www.zeonex.com), were xurographied by a FC8000-60 cutting plotter (Graphtec®, USA, www.graphteccorp.com) and bonded by thermocompression [25]. The device was designed with three inlets (to prevent blocking of the channel with the microspheres) that converge in a 1 mm width channel, 300 μm height, which thinners to 100 μm close to the outlet (Figure 1c-d). The height reduction of the channel enabled to form a weir to pack the microspheres. A small amount of Hyflon AD® powder (Solvay Specialty Polymers), which combines an excellent chemical inertness and optical transparency in water [17][26], was injected prior to the microspheres. The portion of the microfluidic channel filled with the microspheres was 15 mm long. After the microspheres insertion, home-made male connectors that minimize dead-volumes were glued to the device ports. The microfluidic device was proven to resist up to 0.8 bar of pressure during experimental conditions, without leaking. More details on the fluidic setup are provided as ESM, section S2.

2.3 Optical setup and measurement

A custom optical apparatus was used to acquire images of the packed column hosted in the microfluidic device during the flow of samples. The column was illuminated by a red light emitting diode (LED) (Thorlabs, USA, www.thorlabs.com) with peak wavelength $\lambda = 625$ nm and the images were acquired by a charge-coupled device (CCD) camera (Stingray, Allied Technology, Germany, www.alliedvision.com). More details on the optical setup, data acquisition and analysis are provided as ESM in section S3 and S4.

The intensity scattered by the packed column was measured upon flow of deionized water, NaCl water solution, water-ethanol mixtures, water solution of surfactants SDS and benzyldimethylstearylammonium chloride monohydrate (SBSAC) (Sigma-Aldrich). The images captured by the CCD camera at 1 or 0.1 fps were recorded

using a custom LabView program and analyzed using a custom Matlab program. The averaged intensity acquired from a selected region of the packed column was computed as a function of time. The signal S corresponding to the relative increase of scattered light intensity I was computed as:

$$S = \frac{(I - I_0)}{(I_0 - I_f)} \tag{1}$$

where I_0 is the initial intensity measured from microspheres and I_f is the background intensity. The value of I_f was extrapolated from the dependence of I_0 on the solution refractive index n_s, measured for different concentrations of NaCl and assuming $I_0 = I_f$ for $n_s = n_b$, where n_b = 1.331 ±0.002 is the refractive index of the microspheres. The surface coverage of the micro-spheres in the packed column was estimated through the optical scattering model described in [21], which associates the measured increment of scattered intensity S to the thickness h and refractive index n_h of the adsorbed layer by:

$$S = \left(\frac{h}{h^*}\right)^2 \tag{2}$$

where $h^* = k^{-1}|n_b^2 - n_s^2|/|n_h^2 - n_s^2|$, in which k is the scattering vector defined as $k = 4\pi n_s \sin(\theta_s/2)/\lambda$.

3. Results and Discussion

3.1. Microfluidic device assembly

We designed and fabricated a microfluidic column of packed WIM microspheres made of fluoropolymers providing an extraordinary low refractive index. Thanks to this property, the column is largely transparent when filled with water and becomes opaque when a molecular layer adsorbs on the surface of the microspheres, hence acting as a label-free, optical sensor based on the SPI approach. The WIM packed column was assembled by injecting the perfluorinated microspheres into the microfluidic channel (Figure 1). The size and spherical morphology of the microspheres were assessed by optical microscopy, showing a distribution of diameters of 16 ± 4 μm (Figure 1a). Considering the volume of the filled portion of the microfluidic channel (see Materials and Methods), the column contained about 10^6 microspheres. A schematic representation of the microfluidic design is shown in Figure 1c and 1d. The microspheres were introduced into the device through the central inlet using a syringe. The two side inlets were used to remove excess material and trapped air bubbles and were closed after filling. Before each measurement, the column was washed with 30 % (v/v) ethanol for 1 h and then filled with deionized water.

The packed column was highly transparent, when filled with water (Figure 1e and 1f), due to the low refractive index of the microspheres, while it becomes opaque when a flowing solution such as ethanol or salty water (Figure 1g) passed through the column, because of the refractive index mismatch with the microspheres. Remarkably, the intensity of light scattered by the column also increased when kept in index-matching condition with water if molecules adsorbed on the microspheres surface, forming a nanometer-scale layer with different refractive index following the SPI principle. The surface density of adsorbed molecules can be quantified from the increase of scattered light intensity though a suitable optical model [21][27].

3.2. Scattered light intensity increase upon surfactant adsorption on packed microspheres

The opacity of the packed column was measured by a custom imaging setup, described in ESM (section S3). The local changes of opacity as a function of time within the column were extracted by image analysis. An increase of the brightness of the image pixels was associated to an increase of the intensity of light scattered by the corresponding portion of the column. The injection of a sample containing surfactant provided a gradual increase of the opacity of the packed column up to an asymptotic steady state. The subsequent flow of pure water, after the sample solution, induced a decrease of opacity down to about the initial values. From repeated experiments on different microfluidic devices, the signal was recovered after washing within 11 % of its initial value.

We studied the optical response of the forefront region of the column upon injection of two different compounds at the concentration c_a = 30 μM: the cationic surfactant SBSAC and the anionic surfactant SDS. Figure 2 reports the measured adsorption and desorption curves. The asymptotic value of the relative increase of scattered

intensity S computed through Equation 1 was about one order of magnitude larger for the cationic compound relative to the anionic surfactant (see Figure 2 caption). The characteristic time for adsorption and desorption were also very different between the two surfactants, being the absorption kinetic faster and desorption slower for the cationic compound.

The surface coverage of the microspheres in the packed column was estimated from the relative increase of scattered light intensity through Equation 2. Considering a refractive index $n_h = 1.435$ for SBSAC and a molecular length of 2.4 nm estimated from the chemical structure, a compact monolayer of surfactants adsorbed on the microspheres surface corresponds to a scattered intensity increase of about a factor of 10. Therefore, the measured value of S for SBSAC (Figure 2a) corresponds to 50 % of the maximum theoretical surface density of surfactant. In contrast, the smaller measured value of S for SDS (Figure 2b), for which $n_h = 1.461$ and the molecular length is about 1.77 nm, corresponds to only 5 % of the full coverage. The difference between the behaviour of the two surfactants is ascribed to a lower adsorption strength and a smaller surface density of adsorption sites for the anionic compounds on the surface of perfluorinated materials [21]. This is in agreement with previous studies performed on another type of perfluorinated material, Hyflon AD® [21]. Although the proposed method relies on non-specific adsorption, certain chemical selectivity is provided by the different signal amplitude and kinetics observed for cationic and anionic surfactants, as shown in Figure 2. Indeed, the reduced affinity for anionic compounds is ascribed to a general property of fluorinated materials in water: their intrinsic hydrophobicity induces an accumulation of negative charges at the interface with water [28]. In agreement with the study reported in [21], the anionic surfactant also displayed a faster rate for desorption. The data reported in Figure 2c and 3d show that the scattering signal S reached a steady state level much faster for SDS than SBSAC during the washing phase. Remarkably, the rate corresponding to the fast relaxation component of the data in Figure 2c is $1 / \tau_{off} = 6.2 \cdot 10^{-4}$ s^{-1}, which is very similar to the value of $k_{off} = 7 \cdot 10^{-4}$ s^{-1} measured for SBSAC in [21], despite the different composition of the perfluorinated materials.
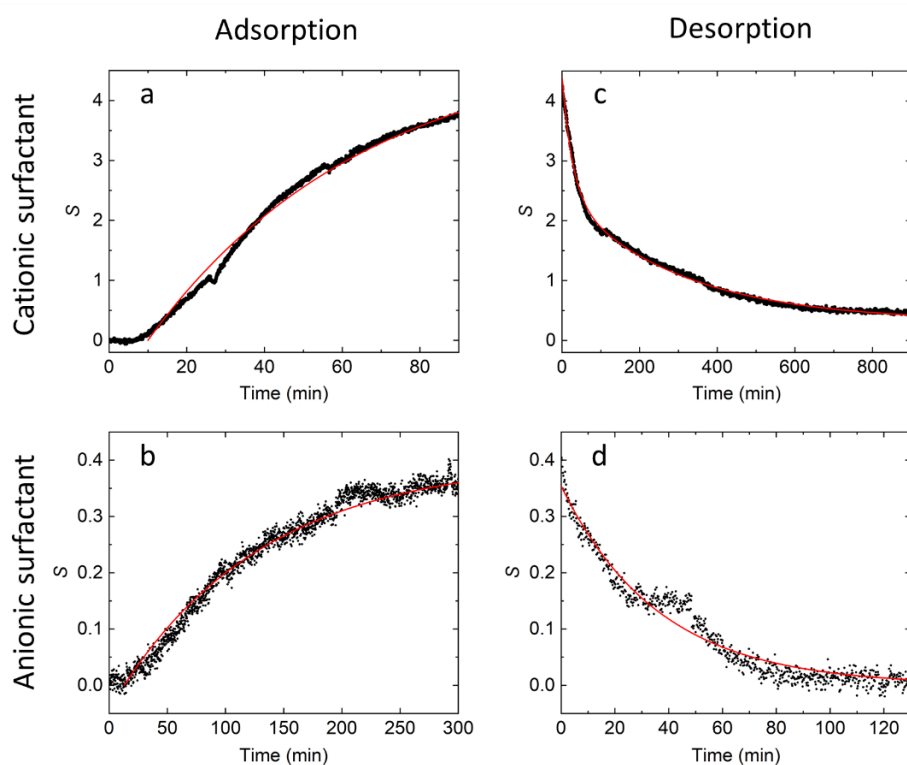

Figure 2. Optical signal from adsorption and desorption of surfactants. Relative increase S of scattered light intensity (black dots) upon injection of surfactant SBSAC (a) and SDS (b) at 30 μM and upon subsequent washing with water (c and d, respectively). The red curves are fitted to single exponential growth or decay functions with amplitude a and time constant τ: $a = 5$ and $\tau = 56$ min (a), $a = 0.4$ and $\tau = 126$ min (b), $a = 0.35$ and $\tau = 36$ min (d). The red curve in (c) is a double exponential fit with amplitudes $a_1 = 1.98$ and $a_2 = 2.12$ and time constant $\tau_1 = 27$ min and $\tau_2 = 301$ min, respectively. In (a) and (b) the fit started at 10 min and 13 min, respectively. Refractive indices of surfactant solutions and water used for washing were 1.333 ±0.001.

3.3. Surfactants delay flow along the column

The proposed packed column design enabled to inspect the adsorption process in real time, along the flow direction, simply measuring the opacity of the column in different subsequent regions of the channel. We observed that the adsorption slowed the flow of surfactants through the packed column relative to the solvent (Figure 3). Figure 3a shows that a sample composed by a water-ethanol mixture provided an increase of opacity due to a change in the refractive index, with a small delay along the column. For a flow rate of 20 µL min^{-1}, considering a bed voidance of about 0.5 [12], the theoretical flow velocity through the packed column is $v_0 = 2$ mm s^{-1} and the minimum theoretical delay across a channel length of 12 mm is 6 s. The observed delay of 40 s is slightly larger, indicating a non-uniform distribution of channel size and streamlines inside the columns. In contrast, if the sample maintains a refractive index similar to that of the washing buffer, but contains molecules that bind to the surface of the microspheres, the scattering signal shows a pronounced delay along the column axis. This effect is clearly shown in Figures 3b-3d, which report the normalized local brightness (see section S4 in ESM), measured at different adjacent regions along the column as a function of time, after injecting 300 µM, 100 µM and 30 µM SBSAC, respectively. Decreasing the surfactant concentration c_a, we observed both, a marked decrease of the growth rate of the optical signal at the column forefront (pink curves) and an increase of the time required to propagate the signal along the column in the direction of the flow.
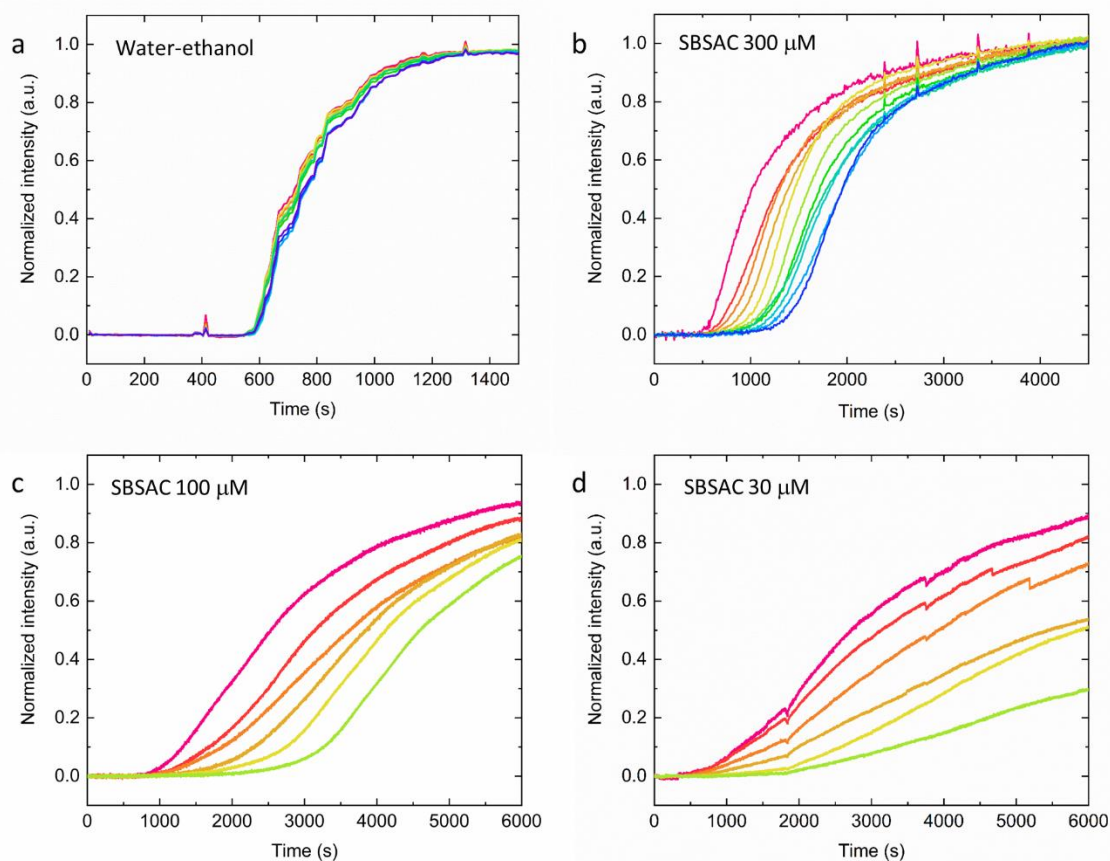

Figure 3. Optical signal measured at different positions along the column. Normalized scattered intensity as a function of time measured during the flow of (a) 50 % (v/v) water-ethanol mixture, (b) 300 µM SBSAC, (c) 100 µM SBSAC, and (d) 30 µM SBSAC. In each panel, the curves represent the optical signal measured in adjacent regions of 1 mm (panels a, b, and c) or 0.8 mm (panel d) length along the packed column. The pink curves correspond to 1 mm from the forefront and the others correspond to consecutive regions according to the same color sequence for all the panels. The time step of the data points is 10 s for panel a and b and 1 s for panel c and d. The value of n_s for water-ethanol (a) is 1.360 ±0.001, whereas of n_s = 1.333 ±0.001 for surfactant solutions (b, c and d).

The access to the measurement of surfactant adhesion on the microspheres and propagation velocity inside the column is granted by the WIM condition. The delay time of the initial growth of the adsorption curves is related to the velocity of surfactants through the streamlines, when the surface of the microspheres is not saturated by the adsorbate yet. Figure 4a reports the delay time as a function of the position along the column and shows a linear dependence for all cases reported in Figure 3, hence indicating constant velocities along the column. For 300 μM SBSAC, we obtained a velocity $v_a = 11.9$ μm s^{-1}, which is much smaller than the velocity $v_0 = 290$ μm s^{-1} of the pure solvent obtained from the data of Figure 3a. Even smaller propagation velocities, 2.6 μm s^{-1} and 1.1 μm s^{-1}, where measured for 100 mM and 300 mM SBSAC, respectively. The signal propagation velocity v_a displayed a linear dependence on surfactant concentration, as reported in Figure 4b.
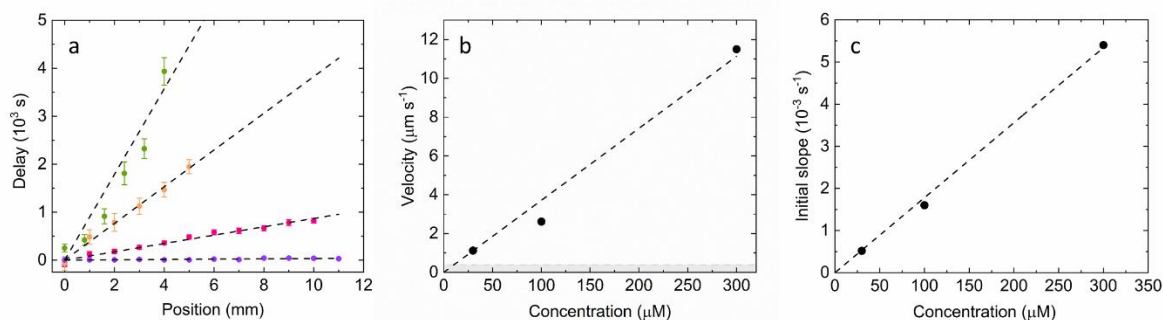

Figure 4. Dependence of optical signal response on SBSAC concentration. (a) Delay of the optical signal along the packed column obtained from the curves of Figure 3. Delay time corresponding to 30 % of the asymptotic amplitude of the intensity curves are reported for 30 μM SBSAC (green), 100 μM SBSAC (orange), 300 μM SBSAC (red), and 50 % (v/v) water-ethanol (violet). Error bars correspond to the effect of intensity noise on the delay time measurement. The dashed lines are linear fits to the data points. (b) Velocities of the optical signal increase along the column obtained from the linear fits of panel a. The dashed line is a linear fit and the grey area represents the uncertainty on the velocity measurement at low SBSAC concentrations. (c) Average speed of growth of the optical signal at 30 % of the maximum amplitude obtained from the SBSAC data of Figure 3.

In general, the velocity v_a observed in presence of adsorption is related to the velocity v_0 through the retention ratio R, as $v_a = Rv_0$. The low values measured for v_a ($R \ll 1$) are consistent with the observation that the surfactant reached the terminal part of the column when the forefront region approached saturation. The dependence of R on the surfactant concentration indicates the amount of molecules retained in a unit volume of the column, which can be expressed as the concentration of binding sites c^*. In case of an ideal packing of microspheres, $R \approx c_a / c^*$, and the slope of v_a vs c_a reported in Figure 4b corresponds to $c^* = 8$ mM, a value much larger than the expected concentration of adsorption sites in the column, 0.4 mM, which was estimated considering an adsorption area per SBSAC molecule of 0.73 nm^2 [21]. The larger value of c^* suggests the presence of void regions in the column, yielding to loss of sample through channelling. The detection performance of the method is expected to get largely improved in case of having an ideal packing of the microspheres.

The delay of the signal-increase along the column represents an analytical parameter that can be converted to concentration values of an unknown sample, through the calibration plot reported in Figure 4b. However, in the current configuration, the precision on the determination of the delay at low concentrations (grey region in Figure 4b) limited the detection to values of 10 μM for the investigated cationic surfactant. A more sensitive analytical parameter is given by the rate of growth of the optical signal at the forefront region of the column, which corresponds to the maximum slope of the pink curves in Figures 3b-3d. Figure 4c shows that the growth rate of the signal normalized to the asymptotic amplitude linearly scales with the surfactant concentration, c_s, with a slope of $1.1 \cdot 10^{-3}$ μM^{-1}min^{-1}. Estimating the background noise as the maximum standard deviation of the baseline $\sigma = 7.5 \cdot 10^{-3}$ observed for the data in Figure 3, the minimum detectable value at 3σ corresponds to a LOD of 1 μM of SBSAC (440 ng mL^{-1}) for a measuring time of 20 minutes. Several methods were proposed to quantify cationic surfactants in water, as summarized in ESM (Table S1), with LODs spread over a large range,

3 ng mL^{-1} [29] - 4 μg mL^{-1} [30]. The method proposed in this work combines a LOD within this range with a microfluidic design and regeneration capability that makes it suitable for online water monitoring platforms.

5. Conclusions

In this work, we demonstrate a novel class of microfluidic chromatography device based on WIM micro-spheres offering the advantage of real time and label-free visualization of binding profiles inside the packed column without fluorescence markers. We show that cationic and anionic surfactants provide different kinetic sensorgrams ascribed to their strength and kinetics of adsorption on the perfluorinated microspheres. The proposed system provided access to a novel analytical parameter, time evolution of the binding profile within the column, through label-free visualisation. The system can be regenerated by washing and is based on a simple optical detection system, which makes it suitable for its integration into compact analytical platforms. The current detection performance is mainly limited by the non-uniform packing of the microspheres. The proposed microfluidic design facilitates the insertion of the microspheres and the removal of air bubbles, which is a major problem in microfluidic packed microcolumns. However, further developments are required to increase the uniformity of the packing and to make the device fabrication protocol suitable for industrial scale production. The selectivity ascribed to adsorption is low, although is enough to discriminate between cationic and anionic surfactants. An increased selectivity can be in principle achieved by including a functionalization step of the microsphere surfaces with specific molecular probes, using approaches previously adopted for other perfluorinated substrates [15].

References

1. Ivanković T, Hrenović J (2010) Surfactants in the Environment. Arch Ind Hyg Toxicol 61:95–110. https://doi.org/10.2478/10004-1254-61-2010-1943
2. Hernández F, Ibáñez M, Portolés T, et al (2015) Advancing towards universal screening for organic pollutants in waters. J Hazard Mater 282:86–95. https://doi.org/10.1016/j.jhazmat.2014.08.006
3. Kutter JP (2012) Liquid phase chromatography on microchips. J Chromatogr A 1221:72–82. https://doi.org/10.1016/j.chroma.2011.10.044
4. Ahmad AL, Low SC, Shukor SRA, et al (2010) Hindered diffusion in lateral flow nitrocellulose membrane: Experimental and modeling studies. J Memb Sci 357:178–184. https://doi.org/10.1016/j.memsci.2010.04.018
5. Malmstadt N, Yager P, Hoffman AS, Stayton PS (2003) A Smart Microfluidic Affinity Chromatography Matrix Composed of Poly(N -isopropylacrylamide)-Coated Beads. Anal Chem 75:2943–2949. https://doi.org/10.1021/ac034274r
6. Jemere AB, Martinez D, Finot M, Harrison DJ (2009) Capillary electrochromatography with packed bead beds in microfluidic devices. Electrophoresis 30:4237–4244. https://doi.org/10.1002/elps.200900334
7. Flemming JH, Baca HK, Werner-Washburne M, et al (2006) A packed microcolumn approach to a cell-based biosensor. Sensors Actuators B Chem 113:376–381. https://doi.org/10.1016/j.snb.2005.03.098
8. Kralj JG, Arya C, Tona A, et al (2012) A simple packed bed device for antibody labelled rare cell capture from whole blood. Lab Chip 12:4972. https://doi.org/10.1039/c2lc41048f
9. Sadavarte R, Madadkar P, Filipe CD, Ghosh R (2018) Rapid preparative separation of monoclonal antibody charge variants using laterally-fed membrane chromatography. J Chromatogr B 1073:27–33. https://doi.org/10.1016/j.jchromb.2017.12.003
10. Ng JK-K, Feng H, Liu W-T (2007) Rapid discrimination of single-nucleotide mismatches using a microfluidic device with monolayered beads. Anal Chim Acta 582:295–303. https://doi.org/10.1016/j.aca.2006.09.016
11. Kim J, Heo J, Crooks RM (2006) Hybridization of DNA to Bead-Immobilized Probes Confined within a Microfluidic Channel. Langmuir 22:10130–10134. https://doi.org/10.1021/la0616956
12. Shapiro MS, Haswell SJ, Lye GJ, Bracewell DG (2009) Design and characterization of a microfluidic packed bed system for protein breakthrough and dynamic binding capacity determination. Biotechnol Prog 25:277–285. https://doi.org/10.1002/btpr.99
13. Cacheux J, Brut M, Bancaud A, et al (2018) Spatial Analysis of Nanofluidic-Embedded Biosensors for Wash-Free Single-Nucleotide Difference Discrimination. ACS Sensors 3:606–611. https://doi.org/10.1021/acssensors.7b00667
14. Zanchetta G, Lanfranco R, Giavazzi F, et al (2017) Emerging applications of label-free optical biosensorsz. Nanophotonics 6:. https://doi.org/10.1515/nanoph-2016-0158

15. Giavazzi F, Salina M, Cerbino R, et al (2013) Multispot, label-free biodetection at a phantom plastic–water interface. Proc Natl Acad Sci 110:9350–9355. https://doi.org/10.1073/pnas.1214589110

16. Giavazzi F, Salina M, Ceccarello E, et al (2014) A fast and simple label-free immunoassay based on a smartphone. Biosens Bioelectron 58:395–402. https://doi.org/10.1016/j.bios.2014.02.077

17. Lanfranco R, Buscaglia M (2016) Invisible Fluorinated Materials for Optical Sensing. In: Reference Module in Materials Science and Materials Engineering. Elsevier

18. Salina M, Giavazzi F, Ceccarello E, et al (2016) Multi-spot, label-free detection of viral infection in complex media by a non-reflecting surface. Sensors Actuators B Chem 223:957–962. https://doi.org/10.1016/j.snb.2015.09.122

19. Zilio C, Bernardi A, Palmioli A, et al (2015) New "clickable" polymeric coating for glycan microarrays. Sensors Actuators, B Chem 215:. https://doi.org/10.1016/j.snb.2015.03.079

20. Nava G, Ceccarello E, Giavazzi F, et al (2016) Label-free detection of DNA single-base mismatches using a simple reflectance-based optical technique. Phys Chem Chem Phys 18:13395–13402. https://doi.org/10.1039/C5CP08017G

21. Lanfranco R, Giavazzi F, Salina M, et al (2016) Selective Adsorption on Fluorinated Plastic Enables the Optical Detection of Molecular Pollutants in Water. Phys Rev Appl 5:054012. https://doi.org/10.1103/PhysRevApplied.5.054012

22. Lanfranco R, Giavazzi F, Bellini T, et al (2020) Fabrication and Optical Modeling of Micro-Porous Membranes Index-Matched with Water for On-Line Sensing Applications. Macromol Mater Eng 305:1900701. https://doi.org/10.1002/mame.201900701

23. van de Hulst HC (1957) Light Scattering by Small Particles. Dover, New York

24. Saez J, Etxebarria J, Antoñana-Diez M, Benito-Lopez F (2016) On-demand generation and removal of alginate biocompatible microvalves for flow control in microfluidics. Sensors Actuators B Chem 234:1–7. https://doi.org/10.1016/j.snb.2016.04.140

25. Saez J, Antonana M, Etxebarria J, Benito-Lopez F (2015) In-situ generated biocompatible alginate actuators for flow control in microfluidics. In: 2015 Transducers - 2015 18th International Conference on Solid-State Sensors, Actuators and Microsystems (TRANSDUCERS). IEEE, pp 2132–2135

26. Merkel TC, Pinnau I, Prabhakar R, Freeman BD (2006) Gas and Vapor Transport Properties of Perfluoropolymers. In: Materials Science of Membranes for Gas and Vapor Separation. John Wiley & Sons, Ltd, Chichester, UK, pp 251–270

27. Lanfranco R, Saez J, Di Nicolò E, et al (2018) Phantom membrane microfluidic cross-flow filtration device for the direct optical detection of water pollutants. Sensors Actuators B Chem 257:924–930. https://doi.org/10.1016/j.snb.2017.11.024

28. Kudin KN, Car R (2008) Why Are Water−Hydrophobic Interfaces Charged? J Am Chem Soc 130:3915–3919. https://doi.org/10.1021/ja077205t

29. Shrivas K, Sahu S, Ghorai A, Shankar R (2016) Gold nanoparticles-based colorimetric determination of cationic surfactants in environmental water samples via both electrostatic and hydrophobic interactions. Microchim Acta 183:827–836. https://doi.org/10.1007/s00604-015-1689-z

30. Öztekin N, Erim FB (2005) Determination of cationic surfactants as the preservatives in an oral solution and a cosmetic product by capillary electrophoresis. J Pharm Biomed Anal 37:1121–1124. https://doi.org/10.1016/j.jpba.2004.07.050

**Electronic Supplementary Material
on the Microchimica Acta publication entitled**

A microfluidic column of water index-matched packed microspheres for label-free observation of water pollutants

Roberta Lanfranco [a], Janire Saez [b], Deborah Abati [a], Thomas Carzaniga [a],
Fernando Benito-Lopez [b,*], Marco Buscaglia [a,*]

*[a] Department of Medical Biotechnology and Translational Medicine, University of Milan,
Italy [b] Microfluidics Cluster UPV/EHU, Analytical Microsystems & Materials for Lab-on-a-
Chip (AMMa-LOAC) Group, Analytical Chemistry Department, University of the Basque
Country UPV/EHU, Barrio Sarriena s/n 48940 Leioa, Spain [*] Corresponding authors.*

S1. Fabrication of water index matched microspheres

We realized a microfluidic column made of packed, water index matched (WIM) microspheres. In order to achieve the WIM conditions, the microspheres were fabricated by fluoropolymers providing an extraordinary low refractive index. This peculiar optical property is granted by the low dipole moment at optical frequencies per unit volume of fluorine-rich compounds. In fact, fluorine is the most electronegative element. In addition to low refractive index, fluorocarbon compounds typically have excellent chemical and thermal resistance compared to hydrocarbon analogues.

The WIM microspheres were fabricated by syringe emulsification followed by UV polymerization of a mix of reactive fluorinated oils. Among those commercially available, we selected two photo-reactive fluoroelastomers, Fomblin MD40 and Fomblin MD700 (Solvay Specialty Polymers, Italy, www.solvay.com), whose refractive indices are slightly smaller (1.295) and slightly larger (1.337) than that of water (1.333), respectively. Furthermore, the selected oils are well miscible and provide reactive groups, which give rise to crosslinking of the polymers upon UV irradiation. After testing different mixtures and measuring the refractive index by an Abbe refractometer, we choose a mixture of 70 % (w/v) Fomblin MD40 and 30 % (w/v) Fomblin MD700, which provided a refractive index of 1.331±0.002. The mixture is immiscible in water, which formed the continuous phase of the micro-emulsion. A surfactant, 4 % (w/v) sodium dodecyl sulphate (SDS) (Sigma-Aldrich, USA, www.sigmaaldrich.com), was added to the continuous phase to stabilize the droplets of fluorinated oils. The micro-emulsion was prepared by the two-syringe emulsification method using membranes with 20 and 50 μm diameter pores (SPG Technology, Japan, www.spg-techno.co.jp). The emulsion was obtained after 20 times back and forth pushing between the two syringes. After emulsification, the product was irradiated for 10 min with a 500 W UV lamp (Helios Italquartz, Italy, www.heliosquartz.com) under gentle agitation to avoid the aggregation of the microspheres. After polymerization, the fraction of largest microspheres or aggregates were discarded through sedimentation.

To facilitate the polymerization reaction, we tested two different photoinitiators: potassium persulfate (Sigma-Aldrich) and Ciba Irgacure 651 (Ciba Specialty Chemicals, Switzerland). Potassium persulfate is soluble in water while Ciba Irgacure 651 is not, and therefore it must be added to the oil phase. Preliminary tests have shown that particles realized with potassium persulfate are not stable over time after UV irradiation. When the emulsion continuous phase is replaced with ethanol, the perfluorinated component undergoes phase separation, hence indicating uncompleted polymerization. In contrast, microspheres produced with Ciba Irgacure 651 remain solid in ethanol for several months after curing. Therefore, 0.1 % (w/v) of this photoinitiator was used to produce the microspheres for the packed column.

S2. Fluidic setup and measurement procedure

The experiments reported in this work were performed using sodium dodecyl sulphate (SDS) or benzyldimethylstearylammonium chloride monohydrate (SBSAC) surfactants (Sigma-Aldrich, USA, www.sigmaaldrich.com) as model samples or 50 % (v/v) water-ethanol mixture as a reference for fluidic characterization. Before each measurement, the surfactants were dissolved in 20 mL pure MilliQ water to the target concentration and 1 mL was used for each experiment.

The fluidic system is composed by a syringe pump (Kent Scientific Genie, Torrington, UK, www.kentscientific.com) and a six-way injection valve (VICI Valco Instruments, www.vici.com), connected to the microfluidic device by silicone tube with diameter 0.5 mm. A 20 mL syringe filled with pure MilliQ water or a water solution with 30 % (v/v) ethanol was connected to the inlet of the chip through the injection valve and driven by the syringe pump at a flow rate of 20 μL min^{-1}. The sample was loaded into a 1 mL loop and connected to the injection valve.

Before each measurement, the packed column was washed with the water-ethanol solution for about 1 h and after washing the pumping syringe was substituted with one containing deionized water. A 30 min baseline was acquired and then the valve was switched to dispense position, the loop was inserted into the circuit and the sample was flowed through the column. The intensity scattered by the packed column was measured during the sample flow. The measurement procedure for real samples obtained from environmental water (*e.g.*, rivers or lake) requires a preliminary mild centrifugation step to discard particulate that can clog the fluidic system and the packed column. The centrifugation step can be substituted by multiple pre-filtering steps for online use in autonomous analytical platforms. A final volume of 1 mL sample is used for each measurement.

S3. Optical setup

The microfluidic device and optical system were placed in a black enclosure to prevent spurious signals from ambient light. The microfluidic device is hosted by a 3D printed holder and connected to the 6-way valve. The images captured by the CCD camera were recorded using a custom LabView program and analyzed using a custom Matlab program. The CCD camera (Stingray, Allied Technology, Germany, www.alliedvision.com) was interfaced with an analog to digital converter, NI USB-9162 Hi Speed USB Carrier (National Instruments, www.ni.com). A custom optical setup was designed and built using opto-mechanical components purchased from Thorlabs (USA, www.thorlabs.com). A schematic representation and a picture of the optical setup are shown in Figure S1. The LED light with peak wavelength of 625 nm passes through a slit providing the shaping of the illumination field, a converging lens at focal distance from an iris to provide control of collimation, and then a second lens that provides an image of the slit on the microfluidic column. The light scattered by the column at 135° relative to the direction of transmitted light is collected by two lenses

forming an image on the CCD plane. Distances between components can be derived from the scale bar in Figure S1b.
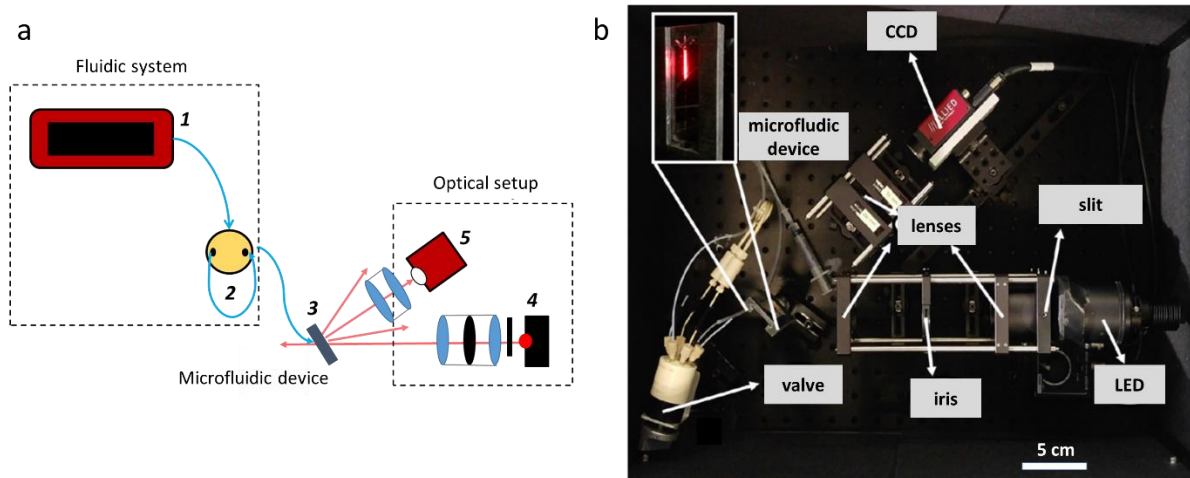

Figure S1. Optical setup for measuring the light scattered by the packed column embedded into the microfluidic device. (a) Schematics of the fluidic and the optical system. The fluidic system is composed by a syringe pump (1) and a six-way injection valve (2), connected to the microfluidic device (3). The channel hosting the packed column of microspheres is illuminated by the light of LED (4) and the scattered light is collected by a CCD camera (5). (b) Image of the optical setup from the top.

S4. Data acquisition and analysis

A simple Labview program was designed to interface the camera and acquire images at a selected and constant frame rate of 1 or 0.1 fps and store them in an automatically generated folder, recording the time of the acquisition. Then, each image in the folder was analyzed with a custom Matlab script in order to study the increment of the scattered light by the microcolumn as a function of both position and time. The main steps of analysis were:

- Load all the images acquired before and during the flow of sample through the packed column.
- Calculate the spatially averaged pixel intensity $I(x,t)$ within identical adjacent image boxes located at position x along the channel (Figure S2) as a function of time t (Figure S3a).
- Compute the average value of $I(x,t)$ for each box before the sample injection (I_0).
- Compute and plot $S(x,t)$, according to Eq. 1.
- Find the time point t_1 at which $I(x,t)$ reaches 30 % of the maximum amplitude for each box.
- Fit $I(x,t-t_1) - I_0$ from $t = t_1$ with exponential growth functions (Figure S3b).
- Compute the maximum value of $S(t)$ from the fitted amplitude, according to Eq. 1.
- Normalize $I(x,t)$ for each box dividing by the fitted amplitude and plot all normalized curves .
- Compute the average slope of the signal increase for each box from the fitting parameter.
- Find the time in which the normalized intensity is equal to 0.3 (delay time).

13

- Plot the delay time of each box as a function of the box position and fit with a linear dependence to obtain the velocity of optical signal propagation along the channel.

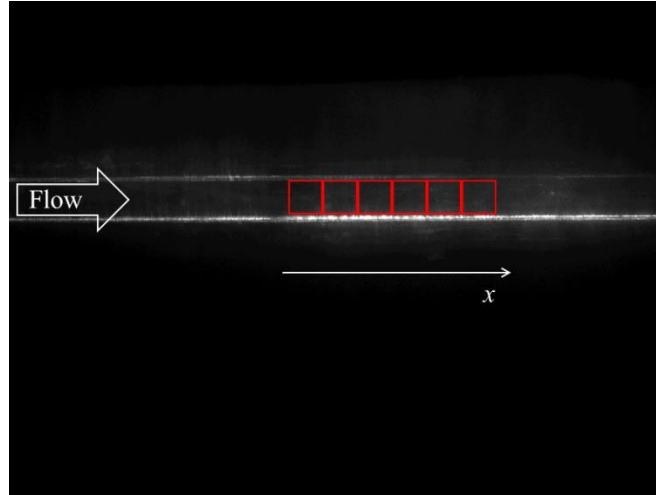The pixel positions in the image corresponding to the column were preliminary defined by visual inspection using ImageJ (https://imagej.nih.gov/ij).

Figure S2. Image of the microfluidic device hosting the packed column of WIM microspheres. The red squares represent the image regions, in which the spatially averaged pixel intensity $I(x,t)$ was computed. The direction of the x coordinate and of the flow is indicated in white.
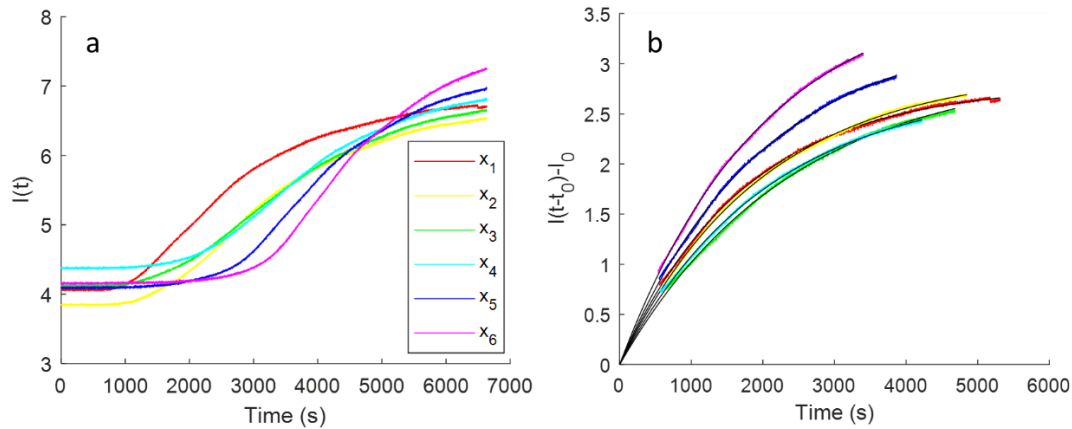

Figure S3. Analysis of image brightness along the microcolumn. (a) The average value of pixels $I(x,t)$ within the boxes at position $x = x_i$ is reported as a function of time. (b) The curves in panel a are reported together with exponential growth fit (black curves). Only the portion of curve above 30% of the total amplitude is shown here and fitted. The time axis is rescaled for each curve according to the initial time extracted from the fit.

S5. Comparison with other techniques

Cationic surfactant are widespread pollutants of water basins and rivers and several methods have been reported for their determination. Table S1 reports a selection of the techniques proposed for the quantification of cationic surfactants in water samples. Most of the methods are based on a laboratory

setting and are not suitable for deployment in autonomous sampling systems. The compact, microfluidic format of the method proposed here, together with the possibility of regeneration of the column by washing with a water-ethanol mixture, makes it suitable for online water monitoring systems. The reported limit of detection (LOD) of the methods reported in Table S1 varies from 3 ng mL^{-1} for gold nanoparticles (AuNPs) probes, up to 4 μg mL^{-1} for capillary electrophoresis. The method proposed here, provides a LOD of 1 μM, corresponding to 440 ng mL^{-1} for SBSAC surfactant, hence within the range of the techniques reported in Table S1. Further improvements of the current LOD are expected by improving the quality of packing of the microspheres in the microfluidic channel and by increasing the size of the column.

Table S1. Overview of recently reported techniques for the quantification of cationic surfactants in water.

Technique	LOD (ng mL^{-1})	Deployable	References
Solid phase extraction–ion chromatography	26	no	[1]
Capillary electrophoresis	4000	no	[2]
Spectrophotometry	110	no	[3]
Matrix-assisted laser desorption ionization mass spectrometry (MALDI-MS)	10	no	[4]
Colorimetric AuNPs Probe	3	no	[5]
Reflective Phantom Interface	40	no	[6]
Phantom membrane microfluidic device	220	yes	[7]
Microfluidic column of WIM microspheres	440	yes	Proposed method

References

1. Olkowska E, Polkowska Ż, Namieśnik J (2013) A solid phase extraction–ion chromatography with conductivity detection procedure for determining cationic surfactants in surface water samples. Talanta 116:210–216. https://doi.org/10.1016/j.talanta.2013.04.083

2. Öztekin N, Erim FB (2005) Determination of cationic surfactants as the preservatives in an oral solution and a cosmetic product by capillary electrophoresis. J Pharm Biomed Anal 37:1121–1124. https://doi.org/10.1016/j.jpba.2004.07.050

3. Agrawal K, Agnihotri G, Shrivas K, et al (2004) Determination of Cationic Surfactants in Environmental Samples by Flow Injection Analysis. Microchim Acta 147:. https://doi.org/10.1007/s00604-004-0228-0

4. Shrivas K, Wu H-F (2007) A rapid, sensitive and effective quantitative method for simultaneous determination of cationic surfactant mixtures from river and municipal wastewater by direct combination of single-drop microextraction with AP-MALDI mass spectrometry. J Mass Spectrom 42:1637–1644. https://doi.org/10.1002/jms.1266

5. Shrivas K, Sahu S, Ghorai A, Shankar R (2016) Gold nanoparticles-based colorimetric determination of cationic surfactants in environmental water samples via both electrostatic and hydrophobic interactions. Microchim Acta 183:827–836. https://doi.org/10.1007/s00604-015-1689-z

6. Lanfranco R, Giavazzi F, Salina M, et al (2016) Selective Adsorption on Fluorinated Plastic Enables the Optical Detection of Molecular Pollutants in Water. Phys Rev Appl 5:054012. https://doi.org/10.1103/PhysRevApplied.5.054012

7. Lanfranco R, Buscaglia M (2016) Invisible Fluorinated Materials for Optical Sensing. In: Reference Module in Materials Science and Materials Engineering. Elsevier